

Article

Analysis and Chromium Recovery from Ferrochrome Waste (Stockpiled Refined Ferrochrome Slags)

Otegen Sariyev ¹, Lyazat Tolymbekova ^{2,*}, Murat Dossekenov ¹, Bauyrzhan Kelamanov ¹, Dauren Yessengaliyev ¹, Assel Davletova ¹ and Assylbek Abdirashit ^{1,*}

¹ Department of Metallurgy and Mining, K. Zhubanov Aktobe Regional University, Aktobe 030000, Kazakhstan; osariyev@zhubanov.edu.kz (O.S.); mdossekenov@zhubanov.edu.kz (M.D.); bkelamanov@zhubanov.edu.kz (B.K.); dyessengaliyev@zhubanov.edu.kz (D.Y.); adavletova@zhubanov.edu.kz (A.D.)

² Department of Chemistry, L.N. Gumilov Eurasian National University, Astana 010008, Kazakhstan

* Correspondence: tolymbekova_lb@enu.kz (L.T.); a.abdirashit@ttu.edu.kz (A.A.); Tel.: +7-707-460-10-20 (A.A.)

Abstract

This study investigates the effectiveness of various beneficiation methods for recovering chromium from refined ferrochrome slag. Dry magnetic separation at different field intensities (0.45 T and 0.8 T) showed that selective extraction of metallic chromium (Cr_{met}) is more efficient at 0.45 T, achieving a recovery rate of up to 90.05%. Pneumatic separation using SEPAIR technology demonstrated promising results, especially for wide particle size fractions (0–20 mm), where chromium recovery reached 40.32% due to density differences between slag particles and metallic inclusions. Enrichment on a shaking table proved to be the most selective method, producing a concentrate with 29.9% Cr and 90.7% recovery, although the yield was low (3.8%). SEM-EDX and SEM-BSE analyses confirmed the heterogeneous phase composition of slag grains, revealing chromium–iron alloys embedded in oxide matrices. Based on laboratory experiments and material characterization, it is concluded that magnetic separation can be used for preliminary concentration, pneumatic classification is effective for processing bulk slag with economic potential, and gravity concentration on shaking tables is suitable for producing high-grade concentrates. The resulting tailings, low in chromium, are suitable for reuse in the production of building materials after carbonation treatment.

Keywords: ferrochrome slags; refined ferrochrome; magnetic separation; chromium recovery; industrial waste; secondary resources; slag processing; metallurgical slags



Academic Editor: Jean François Blais

Received: 16 May 2025

Revised: 21 June 2025

Accepted: 27 June 2025

Published: 30 June 2025

Citation: Sariyev, O.; Tolymbekova, L.; Dossekenov, M.; Kelamanov, B.; Yessengaliyev, D.; Davletova, A.; Abdirashit, A. Analysis and Chromium Recovery from Ferrochrome Waste (Stockpiled Refined Ferrochrome Slags). *Metals* **2025**, *15*, 740. <https://doi.org/10.3390/met15070740>

Copyright: © 2025 by the authors. Licensee MDPI, Basel, Switzerland. This article is an open access article distributed under the terms and conditions of the Creative Commons Attribution (CC BY) license (<https://creativecommons.org/licenses/by/4.0/>).

1. Introduction

The primary use of ferrochrome (85%) is in the production of stainless steel [1]. Stainless steel is used in the manufacture of household goods, kitchen surfaces, and equipment related to food production. According to [2], the flow patterns and in-use stocks of chromium in China's stainless steel production chain from 2012 to 2022 show significant trends. During this period, chromium consumption in China increased substantially, with annual growth rates exceeding 10%, and 90.4% of the chromium was imported. It can be assumed that the demand for chromium will continue to grow in the future. As chromium consumption increases, the production of chromium slags is also expected to rise since these are by-products of chromium extraction and refining processes.

Global ferrochrome slag production ranges between 12 and 16 million tons annually [3].

Depending on the ferrochrome production technology, several types of slag can be generated. Typically, slags are classified into the following categories: high-carbon grades containing 5–8% carbon, medium-carbon grades with 1–4% carbon, and low-carbon (LC) grades containing 0.1–0.5% carbon. The formation of mineral phases in ferrochrome slag systems primarily depends on the slag's chemical composition, as well as the cooling rate or solidification scheme. Additionally, the slag composition is influenced by factors such as ore type, fluxing methods, partial oxygen pressure, reduction temperature, and the residence time of slag in the high-temperature zone of the furnace [4].

Chromium ores used for smelting refined ferrochrome should also contain a minimum amount of silica, which will reduce the consumption of lime, decrease the chromium content of the slag (loss), and increase SiO_2 in the slag. The main amount of low-carbon ferrochrome is produced by silicothermic reduction in chromium oxides using ferrosilichromium in the presence of lime as flux. The reduction in chromium proceeds through $\text{Cr}_2\text{O}_3 \rightarrow \text{CrO} \rightarrow \text{Cr}$. During smelting, other oxides (e.g., silicon, calcium, magnesium, phosphorus, and sulfur) may react to form compounds that enter either the metal or the slag phase, depending on thermodynamic conditions. At the same time, the reduction in oxides of Cr, Si, Ca, Mg, P, S, etc., occurs in the furnace, as evidenced by the presence of these elements in the alloy. Smelting is normally a two-step process: first, only one part of the raw materials (chromite ore, lime, FeSiCr) is loaded into the furnace. After melting that first part, the second part of FeSiCr, chromite ore, and lime are added. As soon as the melting process is completed, metal and slag will be released [5]. The temperature of the slag is 1800 °C, and the temperature of the metal is 1760 °C [6]. The dominant phase in low-carbon chromium slag is γ -dicalcium silicate ($\gamma\text{-C}_2\text{S}$). The main reason for the self-pulverization of refined slag is the polymorphism of the dicalcium silicate; it attains a dusty state during the cooling process after removal from the furnace. When cooled from high temperatures, $\alpha\text{-C}_2\text{S}$ converts to $\beta\text{-C}_2\text{S}$ at 630 °C degrees, then to $\gamma\text{-C}_2\text{S}$ at lower temperatures [7]. Thus, the crumbling feature is caused by the spatial redistribution of close-packed oxygen ions due to changes in ion polarization under the influence of temperature. (N.B. This is the reason why ordinary Portland cement also crumbles.)

Ferrochrome producers in Finland, Sweden, and Russia efficiently utilize these slags in road construction and the production of building materials. In South Africa, ferrochrome slags are safely disposed of in landfills. Due to their excellent combination of high strength and refractory phases, ferrochrome slags can be processed in various ways, including use in road construction, building materials, refractory products, or simply landfilling [8] (Figure 1).

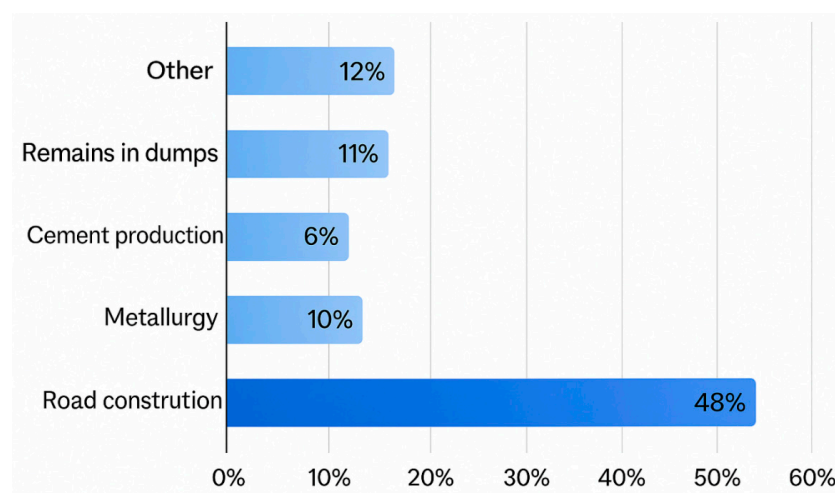


Figure 1. Use of ferrous metallurgy slags in various industries. euros slag.com.

Refined ferrochrome slags are mainly used in the cement industry. However, their application is limited due to the presence of free magnesium oxide and residual chromium oxides, which remain in the mineralogical structure of the slag due to the incomplete reduction in chromium during smelting. These components are strictly regulated by cement industry standards [9].

The depletion of traditional mineral raw materials, combined with the accumulation of industrial waste in long-established metallurgical regions, is having an increasingly harmful impact on both the natural environment and the economic viability of production processes. As natural resources become more scarce, the extraction of new raw materials becomes more expensive and environmentally damaging. At the same time, the waste generated in these industries—such as slags—continues to accumulate, creating environmental threats, especially when not properly managed.

In response to these challenges, interest is growing in exploring the potential of slags as a secondary mineral resource. Slag, a by-product of metallurgical processes, often contains valuable metals and minerals that can be recycled or reused. By finding sustainable methods for slag processing, industries can reduce their dependence on primary raw materials, lessen environmental pressures, and lower production costs. This approach not only facilitates more efficient waste management but also supports the concept of a circular economy—transforming what was previously considered waste into a valuable resource, thereby contributing to more sustainable industrial practices.

For example, ferrochrome dust was used as a partial replacement for conventional silicate in concrete production. Optimal performance was achieved when 40 wt.% of ferrochrome dust and 7 wt.% of lime replaced 47 wt.% of the standard silicate component. Toxicity testing through the TCLP method indicated that the concrete posed no environmental hazards. Therefore, ferrochrome dust presents a sustainable and eco-friendly option for concrete manufacturing [10].

In the study [11], a novel approach was investigated for extracting chromium units from ferrochrome baghouse dust (FeCr BFD) and the ultrafine slag fraction (UFS) using ozonation in an aqueous medium and advanced oxidation processes. The results showed that ozonation in water achieves only limited chromium release from the waste materials. For BFD, the maximum chromium release reached 4.2% of the total content. However, chromium release from BFD was significantly higher compared with the ultrafine slag (UFS), which was attributed to differences in the characteristics of these two materials.

Study [12] examined magnetic and gravity separation methods for concentrating chromium in chromium-containing slags generated during the production of stainless steel (SS) and ferrochrome (FeCr). The results of this research clearly demonstrate the potential of these beneficiation methods for processing SS and high-carbon (HC) FeCr slags. For SS slag, the Wet High Intensity Magnetic Separation (WHIMS) method enabled an increase in chromium concentration to nearly 9 wt.% Cr. Although this chromium content is still too low for ferrochrome production, it may serve as a preliminary step before hydrometallurgical chromium extraction.

The effective separation of iron-bearing components from steel slag using magnetic separation was investigated in [13]. It was concluded that achieving a concentrate with optimal total iron content via dry magnetic separation is a complex task. Therefore, steel slag should undergo multi-stage wet low-intensity magnetic separation with an optimal magnetic intensity of 100 mT.

Magnetic separation is ineffective for recovering iron from fine steel slag particles at magnetic field strengths above 1000 G. Effective separation occurs at fields below 1000 G, particularly in the range of 200 to 800 G. Although lower magnetic field strength increases

the iron content in the concentrate, maintaining higher magnetic field strength in drum magnetic separators is necessary to ensure sufficient product yield [14].

This study focuses on the effectiveness of dry magnetic separation for the recovery of metallic chromium (Cr_{met}) from refined ferrochrome slag, with the aim of quantitatively evaluating the possible recovery rate.

2. Materials and Methods

For this study, we used 48 kg of refined ferrochrome slag. Since the slag sample primarily consists of fine-grained material, no preliminary treatment such as crushing, grinding, milling, or screening was required.

Various methods were employed to characterize and analyze the waste, including particle size distribution, chemical composition, surface chemical composition, and crystalline phase analysis.

Dry sieving was used to determine the particle size distribution of the slag. Microscopic evaluation was performed using a stereomicroscope for detailed microscopic characterization. X-ray powder diffraction analysis (XRD) was applied for phase identification. Additionally, X-ray fluorescence spectrometry (XRF) was used to determine the elemental chemical composition of the sample.

The sample for sieving was homogenized and reduced using the cone and quartering method. The density of the samples was determined according to the LST EN 15103-20107 [15] method using a glass pycnometer. The measured density was 2778 kg/m^3 .

The bulk density of the sample was determined according to the accredited standard method EN 1236-2013 [16]. The bulk density of the material was as follows:

- In a moist state: 1236.1 kg/m^3 ;
- In a dry state: 1122.8 kg/m^3 .

The particle size distribution was determined according to the accredited standard method SRPS ISO 2591-1:1992 [17], using laboratory test sieves made of woven wire cloth and perforated metal plate (Figure 2).

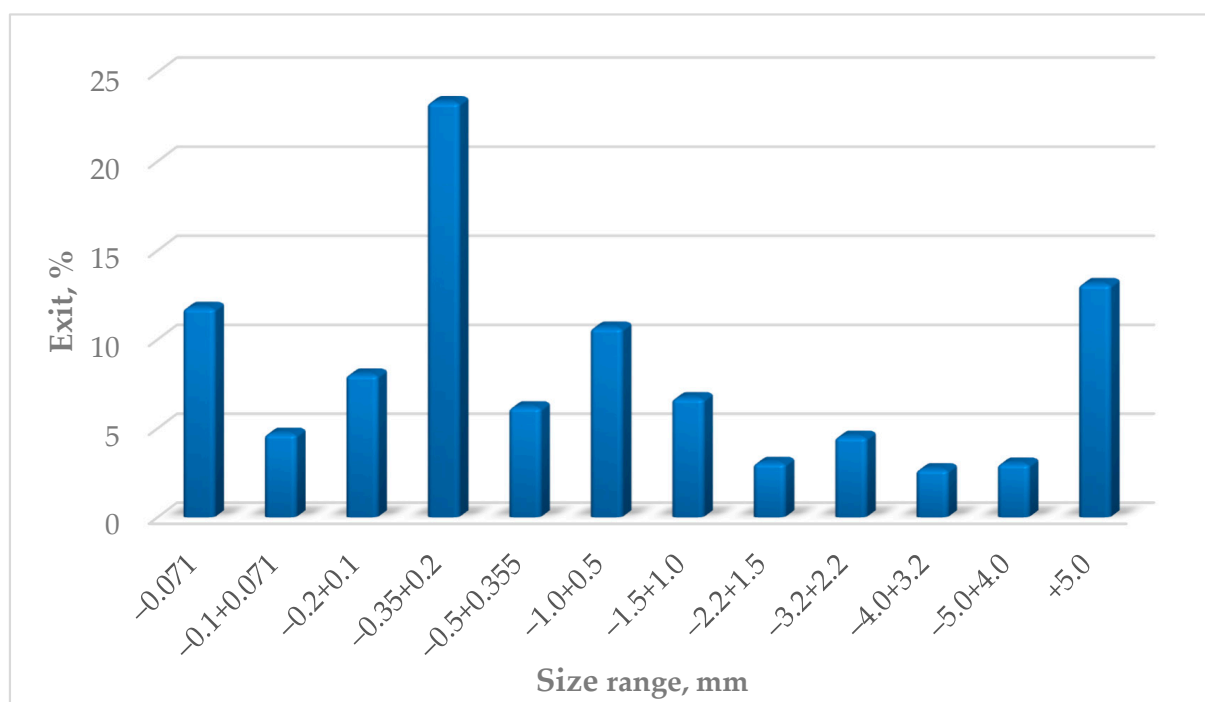
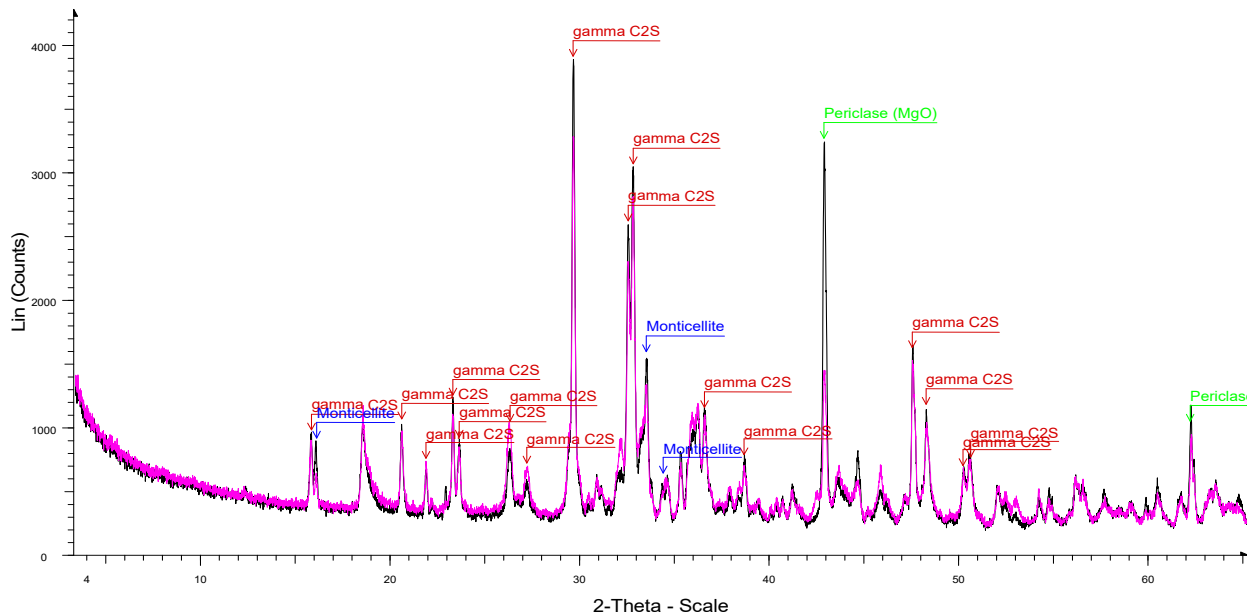


Figure 2. Mass distribution of particle size fractions of the sample determined by the sieving method.

Most of the product appears as a light gray powder, predominantly in the form of aggregated lumps. These lumps easily crumble with minimal effort, turning into a loose powder. Larger grains mainly consist of clusters of small particles of different colors bound together by a grayish powder.

According to the X-ray powder diffraction (XRD) analysis (Figure 3, Table 1), the dominant crystalline phase in the sample is γ -dicalcium silicate (C_2S), indicating a high content of calcium and silicon in the matrix. In addition to γ - C_2S , periclase (MgO) and monticellite—likely iron-substituted and corresponding to the olivine group mineral $Ca(Mg,Fe)SiO_4$ with an orthorhombic structure—were also identified.



Name of mineral	Formula	Bulk slag	Bulk carbonated brick
γ -dicalcium silicate	γ - Ca_2SiO_4	xxx	xxx
Periclase	MgO	xxx	xx
Monticellite	$Ca(Mg,Fe,Mn)SiO_4$	x	x
Magnesiochromite	$MgCr_2O_4$	x	x
Iron-chromium alloy	CrFe	x	x

Legend: x—present; xx—quite abundant; xxx—very abundant.

Figure 3. Detailed X-ray powder diffraction analysis of the sample.

With regard to chromium- and iron-bearing phases, two were clearly detected the following:

- Magnesiochromite ($(Mg,Fe^{2+})(Cr,Al)_2O_4$), a spinel phase, with the majority of its characteristic peaks present in the diffractogram.
- Ferrochrome alloy (CrFe), identified by its most intense diffraction peak at $d = 2.03 \text{ \AA}$, indicating the presence of residual metallic inclusions.

Complementary compositional analysis was performed using wavelength dispersive X-ray fluorescence (WD-XRF). The oxide composition revealed that CaO and SiO_2 dominate, together comprising approximately 60–65 wt.% of the sample. MgO (~8 wt.%) and Al_2O_3 (~3 wt.%) are present as secondary constituents. The total chromium content is approximately 4 wt.%, while iron occurs at lower levels, indicating that chromium is more strongly retained in the residual mineral phases.

Table 1. Semi-quantitative X-ray fluorescence analysis of the examined (submitted) sample.

Component	Weight, %
Major Components	
CaO	44.539
SiO ₂	25.237
MgO	9.029
Cr ₂ O ₃	7.135
MnO	6.731
Al ₂ O ₃	4.521
Fe ₂ O ₃	0.862
Minor Components	
TiO ₂	0.113
Na ₂ O	0.071
SO ₃	0.043
K ₂ O	0.018
NiO	0.018
SrO	0.016
ZnO	0.005
P ₂ O ₅	0.005
Cl	0.014
Trace Components (n.d.—not detected)	
CuO	n.d.
Ga ₂ O ₃	n.d.
As ₂ O ₃	n.d.
Br	n.d.
Rb ₂ O	n.d.
PbO	n.d.
ZrO ₂	n.d.
Bi ₂ O ₃	n.d.

Based on XRD and complementary mineralogical analysis (including optical and SEM-EDS), the following phases were identified in the sample:

- Portlandite, as a hydration product of lime;
- Silicate minerals, including members of the olivine, pyroxene, and amphibole groups;
- Spinel-group minerals, including both natural and secondary chromite and magnesiochromite;
- During solidification, various microstructural features were observed, including garnet minerals, eutectic structures, and sulfide inclusions (e.g., pyrrhotite);
- Limonite, indicative of post-solidification oxidation and weathering;
- Discrete metallic particles representing residual ferrochrome.

The metallic phase content in the sample is estimated to be 2–3 wt.%. It occurs partly as free, rounded particles (beads, spheres) and partly as finely disseminated inclusions encapsulated within silicate matrices, which limits liberation during mechanical processing. Spinel-group minerals were identified as complex solid solutions formed during high-temperature processing.

Given the high proportion of calcium silicate phases, as well as the presence of portlandite, the material—after metallic phase recovery—may be considered as a potential secondary raw material for cement production, pending leaching and mechanical stability evaluations. The portion of the metallic phase embedded in the silicate matrix as mineral chromite is not suitable for magnetic separation.

Considering the grain size fraction found and the natural need to increase recovery of valuable components (freeing the metallic phase included in silicate minerals), the expected usability of metal in the magnetic fraction cannot be high. In other words, low recovery is expected, with a significant portion of metal remaining in the non-magnetic fraction, i.e., in the tails.

2.1. Determination of Metallic and Total Chromium

The quantitative determination of metallic chromium (Cr^0) in the samples was performed in accordance with method MVI 43X-17. This procedure is based on the selective dissolution of metallic phases in diluted hydrochloric acid under controlled temperature and time conditions. The released chromium ions (Cr^{2+}) were then titrated using a standard ferric sulfate (Fe^{3+}) solution. This method allows for the specific quantification of chromium in its metallic state, distinguishing it from oxide and chemically bound forms.

The total chromium content (Cr_{total}) was determined according to method MVI 08X-18, which involves the oxidative fusion of the sample with sodium peroxide or potassium nitrate to convert all chromium compounds into the soluble hexavalent state (Cr^{6+}). The resulting solution was then titrated with a ferrous ammonium sulfate solution to determine the total chromium content. This method ensures that both metallic and oxidized forms of chromium are taken into account.

Both methods were carried out in duplicate to ensure reproducibility and control samples were used to verify accuracy. The results are expressed as a percentage of chromium relative to the initial sample mass.

2.2. Magnetic Separation of Refined Ferrochrome Slag

Preliminary testing is carried out on a laboratory scale using a series of hand magnets with varying magnetic field strengths to determine the efficiency of the process of separating magnetic particles.

Dry magnetic separation experiments were conducted on refined ferrochrome slag using laboratory equipment designed for dry magnetic separation of highly magnetic and weakly magnetic ores and non-metallic materials (0.8 T; 0.45 T). The air classification process was simulated on material sized $-1.0 +0.0$ mm, and the resulting sands were subjected to dry magnetic separation (laboratory separator-analyzer SEM 138-T, NPO “Rudmash”, Saint Petersburg, Russia; 0.55 T).

Prepared samples weighing 100 g each were processed using the DINGS-DAVIS analyzer (Dings Company Magnetic Group, Milwaukee, WI, USA), specifically at three consecutively selected strengths of the inhomogeneous magnetic field, as shown in Figure 4.



Figure 4. Dings–Davis magnetic analyzer with glass tube setup for separation of magnetic and non-magnetic particles in ferrochrome slag samples.

All analyzed samples were further ground to a particle size class of 100% passing 0.5 mm, which is required for the operation of the magnetic analyzer.

On the analyzer, 50 g of the sample was sequentially passed through three non-uniform magnetic fields until the mass of the separated magnetic fraction (MF) reached the amount necessary for chemical analysis.

The experimental setup is shown in Figure 5. In the magnetic separation tests, slags were classified into two groups: magnetic (M) and non-magnetic (NM).

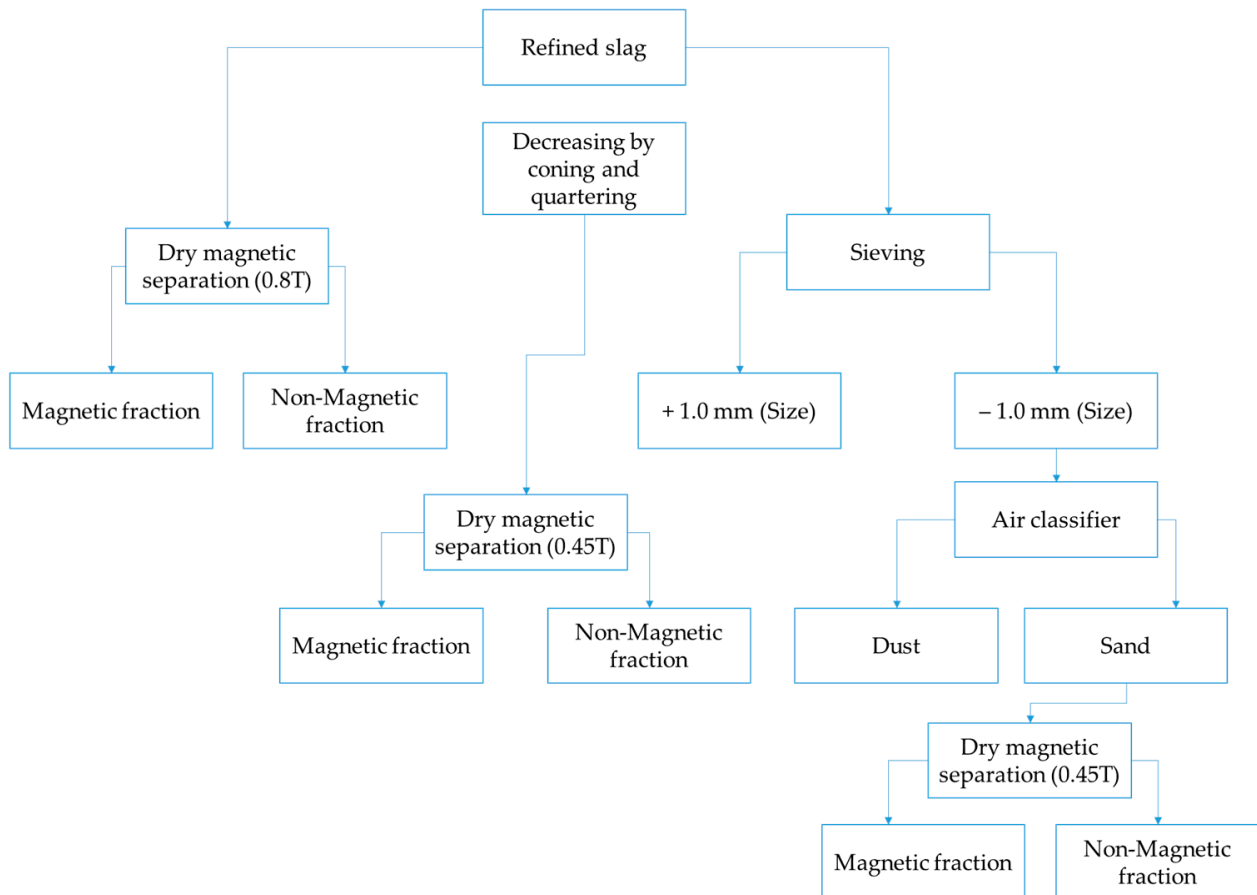


Figure 5. Scheme of the separation of the metallic particle fraction.

2.3. Air Separation

Tests were conducted on a semi-industrial beneficiation plant consisting of a pneumatic separator SEPAIR-1-0.5 (Mechanobr-Tekhnika, Saint Petersburg, Russia), which includes a vibrating feeder, a belt mesh conveyor, a product accumulation hopper, a nozzle, a draft fan DNu-8/1500 (EZTM JSC, Elektrostal, Russia), and an air aspiration system. The setup is shown in Figure 6.

The principle of the separator's operation is as follows: the material fed to the separator is evenly distributed by the vibrating feeder as a uniform layer across the entire width onto the surface of the belt mesh conveyor. While being transported, the material enters the working zone of the nozzle, through which air passes at a certain velocity. The airflow is generated by the operation of a smoke exhaust fan connected via product and slurry separation hoppers to the nozzle. A frequency converter adjusts the operating mode of the draft fan motor and selects the required airflow rate through the nozzle. The ascending airflow imparts an impulse to the material transported along the conveyor. The resulting "lifting" force depends on the shape and density of the materials being separated.



Figure 6. SEPAIR-1-0.5 beneficiation plant.

In the separation zone, a controlled circulating fluidized-like layer is created from material particles with a density equal to the separation density threshold. Particles with a density lower than this threshold for the given airflow will be “captured” and transported to the product hopper, while particles with a higher density will remain on the conveyor and be transported to the accumulation container for the separation tails.

Separation in the air medium is based on a combined characteristic of the particles—density/size/shape. The separation result (quality) depends on the ratio of these factors. By fixing one of the parameters, separation can be conducted according to the others. Since the ultimate goal is to separate the product by density, it is necessary to minimize the influence of size and shape parameters on the separation process. This is achieved by classifying the entire sample into size fractions (machine classes).

Traditionally, tests are performed with size classes of +0–1 mm, +1–3 mm, +3–6 mm, +6–13 mm, +13–25 mm, and +25–50 mm. Size classes above +50 mm are not processed on the existing separation setup due to technological limitations of the laboratory equipment. However, studies on the +50 mm class are conducted by reducing them to smaller classes through crushing. In industrial conditions, the +50–100 mm size class can be enriched using pneumatic separation methods.

2.4. Experiments on the Shaking Table with Refined Ferrochrome Slag

Testing of product separation in water was conducted using beneficiation equipment—a shaking table of the Turkish brand “Merta” with dimensions of 650 × 240 cm. Figure 7 shows the schematic layout of the shaking table device.

Separation of the product in the aqueous medium is based on the combined characteristics of the particles: density, size, and shape. The result (quality) of the separation depends on the ratio of these factors.

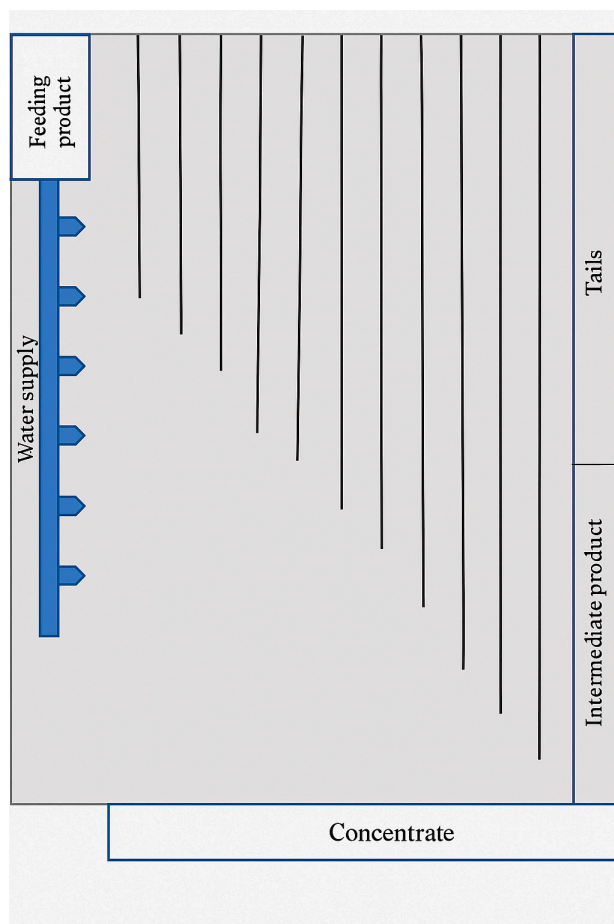


Figure 7. Schematic design of the shaking table.

3. Results and Discussion

The obtained results of magnetic separation are presented in Table 2.

Table 2. Results of dry magnetic separation of refined ferrochrome slag.

Product Name	Yield, %	Content, %		Recovery, %	
		Cr _{total}	Cr _{met}	Cr _{total}	Cr _{met}
Magnetic grains (0.8 T)	72.40	9.00	4.00	79.90	72.06
Non-magnetic grains (0.8 T)	27.60	5.94	4.07	20.00	27.94
Direct chemical analysis	-	6.10	3.60	-	-
Total	100.00	8.16	4.02	100.00	100.00
Magnetic grains (0.45 T)	54.01	11.00	6.70	72.85	90.05
Non-magnetic grains (0.45 T)	54.99	4.81	0.87	27.15	9.95
Direct chemical analysis	-	4.70	1.20	-	-
Total	100.00	8.16	4.02	100.00	100.00

A comparison of the results obtained for dry magnetic separation at different field strengths shows that separation at 0.45 T is more effective for producing cleaner tailings. Specifically, at 0.45 T, the tailings account for approximately 46% of the feed and contain only 0.87% (1.2%) of metallic chromium, indicating a high level of impurity removal. In contrast, tailings obtained at 0.8 T contain significantly higher levels of metallic and total chromium (6.10% and 3.60%, respectively), which contradicts the theoretical expectation of magnetic separation efficiency. According to magnetic separation theory, increasing the magnetic field strength should enhance the recovery of magnetic particles, resulting

in less metal content in the tailings. However, the observed results may be attributed to the heterogeneous nature of metallic inclusions in the slag, where some particles are rich in chromium and others in iron. At higher field strength, Fe-rich particles are more readily captured by the magnet, while Cr-rich particles with lower magnetic susceptibility may remain in the tailings. This explains why increasing field strength does not lead to a proportional increase in chromium recovery. Considering that the primary goal of the preliminary separation stage is to isolate as many final tailings as possible and reduce the load on subsequent processing stages, the use of dry magnetic separation at 0.45 T is considered optimal for this purpose.

Figure 8 shows a metallic bead grain with a heterogeneous phase composition. The SEM-BSE image (Figure 8B) reveals that the grain has a chromium-rich matrix, presumably representing a metallic alloy. SEM-EDX analysis identified dark gray areas on the grain surface, morphologically resembling cubic structures composed of magnesium and oxygen (Mg–O). SEM-EDX also revealed lighter gray regions whose chemical composition (Ca–Si–O) indicates the presence of calcium silicate.

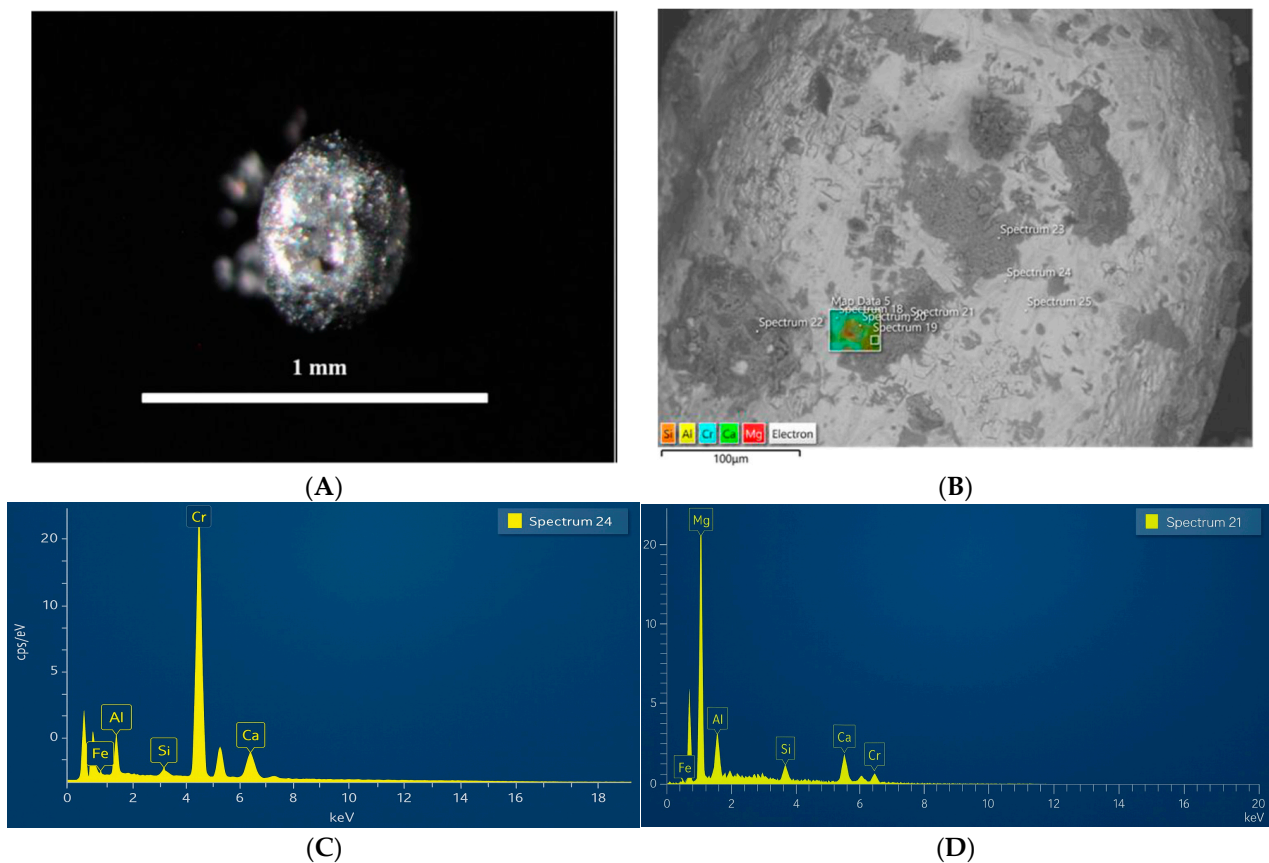


Figure 8. Metallic bead grain with phase composition ((A) Image of the bead obtained using optical microscopy, (B) SEM-BSE image of the metallic bead (alloy), (C) SEM-EDX spectrum (24) of the main matrix composed primarily of chromium (Cr), (D) SEM-EDX spectrum (21) of the dark gray areas consisting of magnesium and oxygen (Mg–O)).

In slag, CrFe typically contains about 0.6–2.2% of metallic inclusions and beads [5], presumably representing a reduced CrFe alloy. For a more detailed study of the magnetic grains, manual selection was carried out. A representative example is shown in Figure 9A, where an alloy grain is presented. The SEM-BSE image (Figure 9B) displays a homogeneous matrix with a smooth surface, and the SEM-EDX spectrum (Figure 9C) shows that the composition consists of chromium and iron (Cr–Fe).

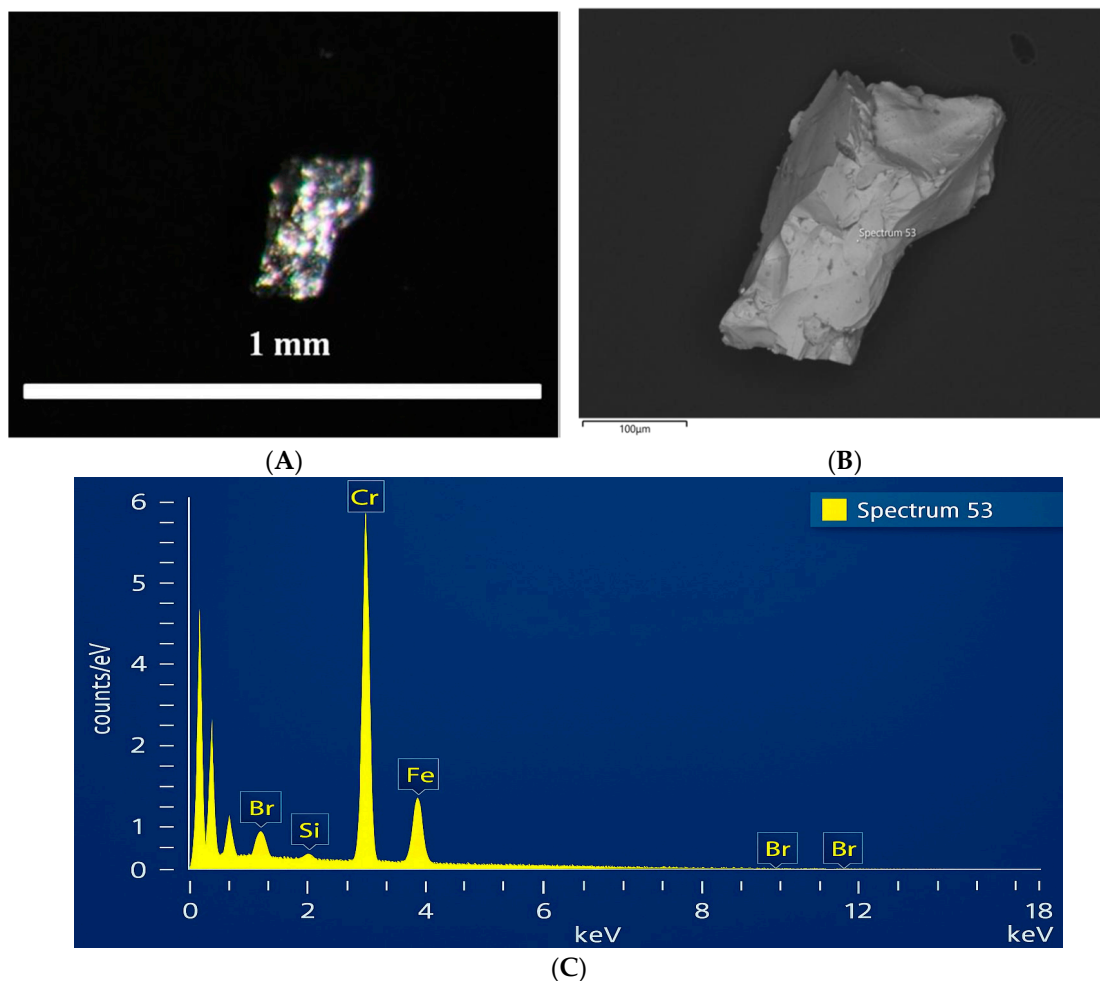


Figure 9. Image of a metallic alloy grain.

In the second stage of the experiment, the initial material was screened through a sieve with a mesh size of 1 mm prior to air classification. The sand fraction obtained after air classification was subjected to magnetic separation at a magnetic field intensity of 0.55 T. The results of the experiment are presented in Figure 10.

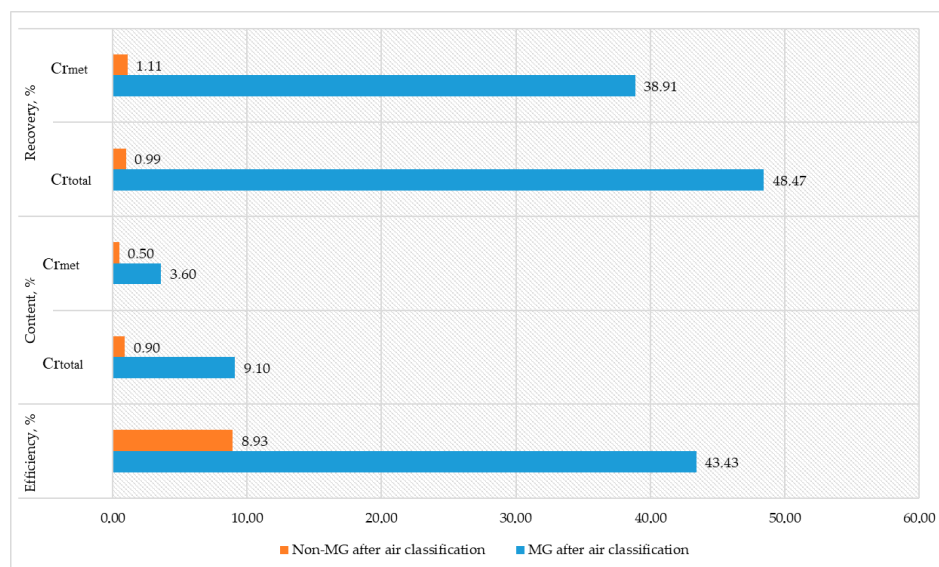


Figure 10. Results of magnetic separation after air classification of refined slag.

Application of Magnetic Separation to Sand Fractions

Magnetic separation of the sand fractions allowed for the recovery of a magnetic fraction containing 3.6% metallic chromium (Cr_{met}), accounting for 83% of the original sand mass, and a non-magnetic fraction with 0.5% Cr_{met} , comprising 17%.

The metallic fraction (MF) obtained after air classification demonstrated a separation efficiency of 43.43%, although it had slightly lower values of total chromium (Cr_{total} —9.10%) and metallic chromium (Cr_{met} —7.70%) compared with the coarser +1 mm fraction (48.47% Cr_{total} and 49.45% Cr_{met}). This indicates that air classification influenced the chromium distribution, likely due to particle size separation, which is supported by data from a scientific study [18].

The non-metallic fraction (non-MF) obtained after air classification exhibited significantly lower efficiency (8.93%) and Cr_{met} content (0.50%), indicating a predominance of non-metallic or low-chromium materials. Recovery values for this fraction were also minimal (1.11% for Cr_{met}), confirming that the majority of valuable chromium remained in the metallic fractions.

The dust fraction constituted a small portion of the total material (4.27%) with relatively low Cr_{total} (3.70%) and Cr_{met} (0.70%) contents. Low chromium recovery values (1.94% for Cr_{total} and 0.74% for Cr_{met}) indicate minimal chromium loss via dust, though this fraction still warrants further investigation. Additional analysis of this fraction could assess the potential for fine material recovery and improve overall chromium utilization.

The study demonstrated that the applied method of dry gravity concentration is effective for enriching the supplied samples of chromium-containing slag.

This segment of the research on slag sample enrichment by pneumatic separation using the “SEPAIR” technology was conducted on size-classified fractions of 0–1 mm, 1–3 mm, 3–6 mm, and a wide size range of 0–20 mm. The Cr content in the initial samples ranged from 1.34% to 1.71%. The qualitative and quantitative parameters of the obtained concentrates, depending on the enrichment depth, are presented in Table 3.

Table 3. Results of the enrichment study using the SEPAIR unit.

Concentrates	Total Yield, %	Cr Content, %	Cr Recovery, %
Class 1–3 mm	1.69	24.58	31.05
Class 3–6 mm			
Enrichment by the wide size class 0–20 mm	3.94	29.12	40.32 *
Size class 1–3, 3–6 and 0–1 mm	2.18	23.64	30.16

* When enriching the wide size class, re-cleaning Product No. 1 (dust 0–1.0 mm) and undersize 0–1.6 mm on a separate separator designed for fine classes can increase recovery by 6–18% or more.

Based on the comparison of the data in this table, it can be concluded that good results were achieved for all particle size classes, regardless of the separation depth.

Nevertheless, the most efficient enrichment was observed when processing the wide particle size class. This is due to the fact that during separate classification, materials larger than 6 mm were not involved in the enrichment process. Re-cleaning Product No. 1 (dust 0–1.0 mm) and undersize 0–1.6 mm on a separator for fine fractions can increase recovery up to 69% or more.

The high efficiency of enrichment using the wide particle size class without prior size classification is attributed to the significant density difference between the slag particles and the metallic droplets. This is a clear advantage, as industrial-scale enrichment would not require a separate separator for each size class.

The industrial products obtained from enrichment, with chromium content ranging from 1.8% to 5.5%, can be subjected to re-cleaning for additional chromium recovery after further crushing.

Enrichment of refined ferrochrome slag using a shaking table effectively separated the chromium-containing fraction as a concentrate. Despite the small mass yield of the concentrate (only 3.8% of the total mass), its chromium content was high—29.9%, ensuring a 90.7% total chromium recovery. This indicates the high selectivity of the separation by density and particle size. Such a result is especially valuable in waste processing, where minimizing the loss of valuable components is crucial.

The main portion of the material (93.2%) was discarded as tailings with a very low chromium content—0.2%. Their contribution to total recovery was only 8.1%, confirming the effective concentration of the valuable phase in the heavy fraction. The intermediate product, accounting for 3.1% of the mass, had a chromium content of 0.4% and an insignificant contribution to recovery—1.2% (Table 4). Figure 11 visually illustrates the separation of products on the shaking table, confirming the high-quality sorting of the material.

Table 4. Results of slag enrichment on the concentration table.

Product	Mass, kg	Yield, %	Cr Content, %	Cr Recovery, %
Tails	15.0	93.2	0.2	8.1
Intermediate product	0.5	3.1	0.4	1.2
Concentrate	0.6	3.8	29.9	90.7
Total	16.1	100.0	2.2 (Average)	100.0



Figure 11. Distribution of products on the concentration table.

The concentrate obtained on the concentration table contained several green, spherical grains with an uneven surface texture. At high magnification under SEM-BSE, a heterogeneous matrix was revealed, with black spots surrounded by a lighter pattern (Figure 12). A bright gray pattern of various shapes is observed: some are rounded, while others are elongated. The black cubic-shaped spots are enriched with magnesium (Figure 12D). This phase may correspond to periclase (MgO), which is supported by XRD analysis results. Elemental mapping analysis (Figure 12B) shows that the gray areas consist of Ca-Si-O, presumably dicalcium silicate (Ca_2SiO_4), which was identified in the XRD analysis. Between them, a small transition zone of Ca-Mg silicate is assumed.

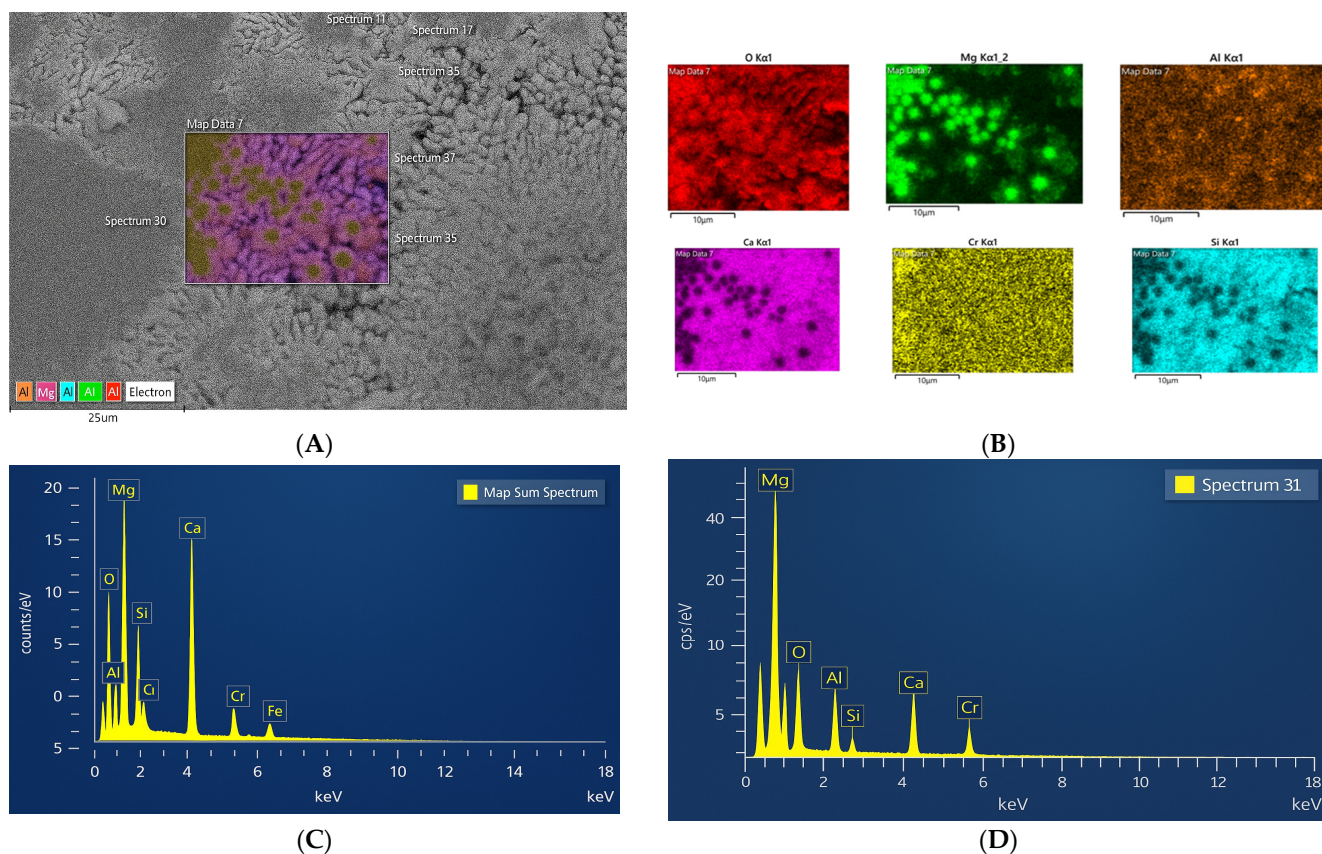


Figure 12. Microstructure and elemental analysis of the slag grain: (A) Image of the grain at higher magnification using SEM-BSE; (B) Mapping of the selected fine-grained matrix: pink color indicates larnite (pink for Ca, blue for Si, and red for O), and greenish color indicates magnesium oxide (green for Mg and red for O); (C) SEM-EDX analysis of the grain matrix; (D) SEM-EDX analysis of spectrum 31, consisting mainly of Mg-O. Al and Cr are present in minor amounts throughout.

4. Conclusions

The results of both magnetic separation and pneumatic classification highlight the effectiveness of different separation methods for concentrating chromium (Cr).

Magnetic separation: At a magnetic field intensity of 0.8 T, most of the material (72.40%) passes into the magnetic fraction, but the distribution of metallic chromium (Cr_{met}) between the magnetic and non-magnetic fractions is almost equal, which reduces the efficiency of extracting metallic chromium. At 0.45 T, although less material (54.01%) enters the magnetic fraction, the Cr_{met} content is significantly higher (6.70%), and the extraction of Cr_{met} reaches a much higher level—90.05%.

According to these results, the 0.45 T mode is more effective for selective concentration of metallic chromium, while 0.8 T captures more total material but with lower selectivity.

Combination of pneumatic classification and magnetic separation: This can optimize chromium recovery. Pneumatic classification effectively concentrates chromium in the metallic fraction, while magnetic separation at 0.45 T is especially efficient for the selective extraction of metallic chromium.

Pneumatic separation using the “SEPAIR” technology: This method demonstrated high efficiency in enriching chromium-containing slags, especially when processing a wide size fraction (0–20 mm), which allowed chromium recovery up to 40.32%. This is due to the involvement of larger particles in the process, thanks to the significant difference in densities between slag grains and metallic particles. Also, using a single separator for a wide fraction reduces costs and simplifies the technological process.

Enrichment on a concentration table: The process showed high selectivity, producing a concentrate with a chromium content of 29.9% and a recovery of 90.7%. Despite the low concentrate yield (only 3.8% of the total mass), the process effectively separated the chromium-containing fraction, minimizing losses of valuable components. Such results confirm the high efficiency of both methods for slag processing, contributing to improved final product quality and overall profitability.

Comparison of methods: The highest chromium content concentrate can be obtained via processing on the concentration table, although the yield is low. Dry magnetic separation at 0.45 T provided 72.85% product extraction as magnetic particles with a total chromium content of 11% and an efficiency of 54.01%.

Based on the studies of mechanical, mineralogical, and chemical properties of the raw material—slag—as well as laboratory testing of various enrichment methods, the following conclusions can be made:

- Magnetic separation/enrichment methods, due to their low extraction and enrichment degrees, can be applied as primary processing methods.
- Pneumatic separation shows satisfactory results, and the concentrates obtained can already be economically justified as feedstock for remelting and production of commercial ferrochrome.
- Enrichment on concentration tables allows for maximum extraction of the valuable component as concentrates are suitable for remelting and for direct use after briquetting.

The tails obtained can be used as raw material for producing shaped construction products subjected to autoclave carbonation with carbon dioxide [19].

Author Contributions: Conceptualization, O.S. and M.D.; methodology, B.K. and A.A.; software, A.A. and B.K.; validation, D.Y., A.D. and A.A.; formal analysis, A.D. and M.D.; investigation, A.D. and D.Y.; resources, A.D.; data curation, A.A.; writing—original draft preparation, O.S. and L.T.; writing—review and editing, O.S., B.K., D.Y. and L.T.; visualization, A.A.; supervision, A.D.; project administration, O.S.; funding acquisition, O.S. All authors have read and agreed to the published version of the manuscript.

Funding: This research is funded by the Science Committee of the Ministry of Science and Higher Education of the Republic of Kazakhstan (Grant No. AR 19577218).

Data Availability Statement: The original contributions presented in this study are included in the article. Further inquiries can be directed to the corresponding authors.

Acknowledgments: The authors declare that no generative AI tools were used for text generation, data analysis, or any part of the study design or manuscript preparation.

Conflicts of Interest: The funders had no role in the design of the study; in the collection, analyses, or interpretation of data; in the writing of the manuscript; or in the decision to publish the results.

References

1. Cunat, P. *Alloying Elements in Stainless Steel and Other Chromium-Containing Alloys*; International Chromium Development Association: Paris, France, 2004; pp. 1–24. Available online: <http://scholar.google.com/scholar?hl=en&btnG=Search&q=intitle:Alloying+Elements+in+Stainless+Steel+and+Other+Chromium-Containing+Alloys> (accessed on 25 January 2025).
2. Yang, L.; Liu, J.; Hua, X.; Wang, H. Mapping Chromium Flows in China’s Stainless-Steel Product Chain: A Product-Level Substance Flow Analysis. *Resour. Conserv. Recycl.* **2024**, *209*, 107816. [[CrossRef](#)]
3. Richard, P. Overview of the Global Chrome Market. In Proceedings of the INDINOX Stainless Steel Conference-1, Ahmedabad, India, 25–26 January 2015.
4. Hayes, P.C. Aspects of SAF Smelting of Ferrochrome. In Proceedings of the Tenth International Ferroalloys Congress, Cape Town, South Africa, 1–4 February 2004; pp. 1–14.
5. Gasik, M.I. Technology of Chromium and Its Ferroalloys. In *Handbook of Ferroalloys*, 12th ed.; Elsevier: Amsterdam, The Netherlands, 2013. [[CrossRef](#)]
6. Ryss, I. **Recovery Methods for Metallurgical Slags**; Metallurgy Press: Moscow, Russia, 1985. (In Russian)
7. Chang, Q.; Smith, J.; Liu, H. Investigation of Chromium Recovery Techniques from Ferrochrome Slag. *Metall. Mater. Trans.* **2016**, *47*, 1234–1245.
8. Sahu, N.; Biswas, A.; Kapure, G.U. A Short Review on Utilization of Ferrochromium Slag. *Miner. Process. Extr. Metall. Rev.* **2016**, *37*, 211–219. [[CrossRef](#)]
9. Sariyev, O.R.; Musabekov, Z.B.; Dossekenov, M.S. Disposal of Slag of Refined Ferrochromium by Obtaining a Sintered and Carbonized Construction Products. *Kompleks. Ispolz. Miner. Syra = Complex Use Miner. Resour.* **2019**, *4*, 26–34. [[CrossRef](#)]
10. Acharya, P.K.; Patro, S.K. Use of Ferrochrome Ash (FCA) and Lime Dust in Concrete Preparation. *J. Clean. Prod.* **2016**, *131*, 237–246. [[CrossRef](#)]
11. Van Staden, Y.; Beukes, J.P.; Van Zyl, P.G.; Du Toit, J.S.; Dawson, N.F. Characterisation and Liberation of Chromium from Fine Ferrochrome Waste Materials. *Miner. Eng.* **2014**, *56*, 112–120. [[CrossRef](#)]
12. Kukurugya, F.; Nielsen, P.; Horckmans, L. Up-Concentration of Chromium in Stainless Steel Slag and Ferrochromium Slags by Magnetic and Gravity Separation. *Minerals* **2020**, *10*, 906. [[CrossRef](#)]
13. Liu, X.; Wang, D.Z.; Li, Z.W.; Ouyang, W.; Bao, Y.P.; Gu, C. Efficient Separation of Iron Elements from Steel Slag Based on Magnetic Separation Process. *J. Mater. Res. Technol.* **2023**, *23*, 2362–2370. [[CrossRef](#)]
14. Ma, N.; Houser, J.B. Recycling of Steelmaking Slag Fines by Weak Magnetic Separation Coupled with Selective Particle Size Screening. *J. Clean. Prod.* **2014**, *82*, 221–231. [[CrossRef](#)]
15. *LST EN 15103:2017*; Furniture—Storage Units—Safety Requirements and Test Methods. Lithuanian Standards Board (LST): Vilnius, Lithuania, 2017.
16. *EN 1236:2013*; Copper and Copper Alloys—Method for Determination of Lead Content—Flame Atomic Absorption Spectrometric Method. European Committee for Standardization (CEN): Brussels, Belgium, 2013.
17. *SRPS ISO 2591-1:1992*; Test Sieving—Part 1: Methods Using Test Sieves. Institute for Standardization of Serbia: Belgrade, Serbia, 1992.
18. Alanyali, H.; Çöl, M.; Yilmaz, M.; Karagöz, Ş. Application of Magnetic Separation to Steelmaking Slags for Reclamation. *Waste Manag.* **2006**, *26*, 1133–1139. [[CrossRef](#)] [[PubMed](#)]
19. Sariyev, O.; Kelamanov, B.; Dossekenov, M.; Davletova, A.; Kuatbay, Y.; Zhuniskaliyev, T.; Abdirashit, A.; Gasik, M. Environmental Characterization of Ferrochromium Production Waste (Refined Slag) and Its Carbonization Product. *Heliyon* **2024**, *10*, e30789. [[CrossRef](#)] [[PubMed](#)]

Disclaimer/Publisher’s Note: The statements, opinions and data contained in all publications are solely those of the individual author(s) and contributor(s) and not of MDPI and/or the editor(s). MDPI and/or the editor(s) disclaim responsibility for any injury to people or property resulting from any ideas, methods, instructions or products referred to in the content.